ICARUS 77, 414–438 (1989)

Observations of the $J = 1–0$ CO Lines in the Mars Atmosphere: Radiodetection of ^{13}CO and Monitoring of ^{12}CO

E. LELLOUCH,* M. GÉRIN,† F. COMBES,† S. ATREYA,‡ AND T. ENCRENAZ*

*Département de Recherches Spatiales, Observatoire de Paris-Meudon, 92195 Meudon Principal Cedex, France; †Laboratoire de Radio Astronomie Millimétrique, Ecole Normale Supérieure, 24, rue Lhomond, 75005 Paris, France; and ‡Department of Atmospheric, Oceanic and Space Sciences, University of Michigan, Ann Arbor, Michigan 48109-2143

Received November 4, 1987; revised June 10, 1988

Repeated millimeter-wave observations of Mars, performed in September and October 1986 and January 1987, allowed a high-resolution recording of the $J = 1–0$ ^{12}CO line, and the first radiodetection of ^{13}CO. In the hypothesis where the thermal profile has the structure measured by the *Viking* spacecrafts, our observations are not compatible with a terrestrial $^{12}C/^{13}C$ isotopic ratio. If the isotope ratio is assumed terrestrial, then the observations imply that the thermal profile is very different from the profile in dust-free conditions, especially in its lower part, and that the CO abundance could vary by a factor of about 2 over a period of a few months.

I. INTRODUCTION

Carbon monoxide is a key molecule for understanding the aeronomical processes and the stability of the Mars atmosphere. Photodissociation of CO_2 yields CO and O. Atomic oxygen reacts with itself in a three-body recombination reaction to form O_2. Yet, since the detection of CO at 1.6 and 2.4 μm (Kaplan *et al.* 1969), microwave observations revealed CO abundances below predicted levels by orders of magnitude. Hunten (1974) suggested that catalytic recombination of CO and O_2 to CO_2 might be variable in time and predicted short-term (2 years) variability of O_2 and CO. As will be explained later, the stability of the Martian CO_2 is best explained by another mechanism which also could imply a temporal or sporadic variability. The CO abundance is likely to be variable (Good and Schloerb 1981, Clancy *et al.* 1983), but a problem remains as O_2 is not variable (Trauger and Lunine 1983), and further investigations on CO variability are needed.

The original observation by Kaplan *et al.* (1969) also led to the detection of ^{13}CO. The measurement was compatible with a terrestrial $^{12}CO/^{13}CO$ ratio. Since this detection, no other observation of ^{13}CO was reported.

Thermal profiles of Mars have been measured during the *Viking* 1 and 2 descents (Seiff and Kirk 1977). The *Viking* landers also measured the optical depth of the dust suspended in the atmosphere at two sites versus time during nearly an entire Martian year. Pollack *et al.* (1979) modeled the physical properties of dust and its effects on the thermal profile and, taking into account dynamical effects, were able to reproduce the thermal profile observed by the *Viking* probes.

Millimeter-wave observations of planets are of high interest because the high resolution provided by the heterodyne technique allows one to probe the atmosphere up to the most tenuous layers. The vertical distribution of the minor constituents and/or the thermal profile can be inferred from the shape of the microwave lines (Schloerb 1985, Lellouch and Encrenaz 1986).

We report here repeated observations of Mars at ^{12}CO and ^{13}CO $J = 1–0$ line frequencies, performed shortly after the 1986

0019-1035/89 $3.00

opposition. The first radiodetection of ^{13}CO was achieved, and the observed ^{12}CO lines showed significant temporal evolution. Section 2 describes the observations. Section 3 describes the data reduction. Results are presented and discussed in Section 4.

2. OBSERVATIONS

In September and October 1986, and January 1987, we observed the $J = 1–0$ transitions of ^{12}CO at 115.271 GHz and ^{13}CO at 110.201 GHz in the atmosphere of Mars. The observations were made with the IRAM (Institut de Radio Astronomie Millimétrique) 30-m telescope at Pico Veleta near Granada, Spain. The telescope beam size was 22″ at the ^{12}CO (1–0) frequency and 23″ for ^{13}CO. We checked the pointing on Mars by broadband continuum observations, before the starting of line observations. The rms pointing error was less than 5″.

We used a SIS receiver for the ^{12}CO observations, and a Schottky receiver for the ^{13}CO observations. All observations were made in double signal sideband (DSB) mode, with a band separation of 7840 MHz. Spectra were recorded using the usual calibration procedure: all spectra were taken in position switching mode, with reference position 6′ away from the source, well outside the diffraction pattern of the telescope. The integration time for each individual scan was 5 min, made of 5 pairs of 30-sec on-source and 30-sec off-source integrations. Chopper wheel calibrations were done at the beginning of each scan. The total system temperature outside the atmosphere was typically $T_{sys} = 2000$°K. At the CO frequency, the aperture efficiency of the telescope is 0.36, the telescope efficiency η_l is 0.87 (Kutner and Ulich 1981), and the forward scattering and spillover efficiency is 0.78. The antenna temperature scale used throughout this paper will be T_R^*, the antenna temperature corrected for all losses in the atmosphere and the antenna including spillover.

The DSB mode introduces difficulties in the calibration procedure because the gain of the receiver and the atmospheric opacity vary from one sideband to the other (the latter is especially serious between 115.27 and 107.43 GHz). However, the gain of the receiver in each band had been previously measured by adding a filter to reject the image sideband (M. Guelin, private communication). The calibration system at IRAM uses an atmospheric model that allows one to evaluate atmospheric opacity in the two sidebands and accounts of course for the air mass of the sources (Guelin *et al.* 1986). This removes most of the error introduced by the difference in opacity in the two bands, but some residual uncertainty related to local "meteorological" conditions cannot be avoided. As a further check, we observed CO lines DR21 and IRC2 in Orion, and concluded that the line calibration was satisfactory to 10–15%.

For spectral analysis, we used two filter banks: one of 512 contiguous 1-MHz channels, and one of 256 contiguous 100-kHz channels, centered on Mars' velocity, to investigate in detail the ^{12}CO absorption line.

A careful study of the individual scans recorded in a given observation sequence showed that the continuum levels (i.e., the antenna temperatures measured far away from the center of the line) vary from one scan to another by as much as 10°K. This is likely due to changing atmospheric conditions during the observation sequence. This is not too serious for the September 1986 spectra, for which the antenna temperature at Mars was about 100°K. For October and January spectra in contrast, due to much less favorable filling factors (see Table I), the antenna temperatures at Mars were about 50 and 20°K, respectively. The fluctuations in the antenna temperatures become then too important to achieve a reliable determination of the Mars continuum level. Therefore, we think that, instead of measuring the line-to-continuum ratio, as is usually done in millimeter-wave spectroscopy of planets, the observations provide a satisfactory (although limited by the line

TABLE I

SUMMARY OF OBSERVATIONAL PARAMETERS

Date of observation	9–12 Sept. 1986	23 Oct. 1986	21 Jan. 1987
Mars' apparent diameter	16"1	11"3	6"2
Filling factor	0.30	0.16	0.05
Solar longitude	242°	268°	322°
Subearth point			
Latitude	6 S	16 S	25 S
Local hour	9:30	9:00	9:20

calibration accuracy) determination of the line "absolute" characteristics (i.e., height in °K) and only a poor estimate of the continuum level.

Figures 1 to 3 show our total averaged spectra, after removal of first or second degree baselines and correcting for the dilution factor, assuming a Gaussian beam. (Note that the Schottky receiver was not available in October; neither was the 100-kHz filterbank in January.) Removal of second degree baselines does not modify the shape of the lines, because the frequency scale of the baseline ripples is much greater than the typical variation scale of the lines (500 MHz vs 100 MHz for ^{12}CO and 20 MHz for ^{13}CO). To give an idea of the quality of the baseline, we also show the raw (averaged) ^{12}CO spectrum recorded in September 1986. We believe that these spectra show the intrinsic line-to-continuum contrasts (in brightness temperature) at the planet and that a conservative approach is to assume a precision on the calibration of 15%. Clearly, the observed ^{12}CO lines show a temporal evolution, as will be discussed below. Although detected on every individual scan, the ^{13}CO line recorded in September shows up only marginally from the noise level and could be an artifact due to baseline ripples on the raw spectra. This is why the experiment was repeated in January 1987, showing unambiguously the first radiodetection of ^{13}CO on Mars. The poor S/N on the ^{12}CO January spectrum is due to a short integration time (5 min).

As seen in Figs. 1 to 3, the ^{12}CO lines exhibit an interesting structure of broad emission wings, with a narrow (5 MHz) absorption core. As noted by Good and Schloerb (1981), the emission in the wings is due to the fact that the brightness temperature of the surface, which is the product of the physical surface temperature by its emissivity, is lower than the kinetic temperature of the gas just above it. ^{12}CO in the lower atmosphere is seen in emission against the colder background of the surface. Near the center, the ^{12}CO opacity is larger, and the weighting function peaks in the cold upper atmosphere: the core is seen in absorption. The ^{13}CO line is only seen in emission because, due to the low ^{13}CO mixing ratio, the weighting function peaks always near the surface.

Apart from the fact that our bandwidth is larger, ensuring proper definition of the baseline, and our resolution better (0.1 MHz), the main difference between our observed ^{12}CO lines and Good and Schloerb's (1981) lies in a much greater emission-to-absorption ratio in all our lines. The bandwidth used in their observation (256 MHz) is comparable with the total width of the line. The faint emission wings will therefore disappear in the baseline, resulting in an enhanced absorption-to-emission ratio in their spectrum. This observational effect, and differences in the thermal profile, probably explain the different lineshapes of their spectra and ours.

As we said, the planetary disk was not resolved in the observations. Some important orbital parameters of Mars are summarized in Table I. Note that September and October observations were done very close to perihelion (25 September 1986), a period favorable for major dust storms (Martin 1974). A major dust storm was expected for a period of a few months starting in July 1986 (Martin and James 1987). However, amateur observations revealed no global dust storm during fall 1986 or early 1987, although there were numerous small storms, particularly in Hellas, throughout the period (P. James, private communication).

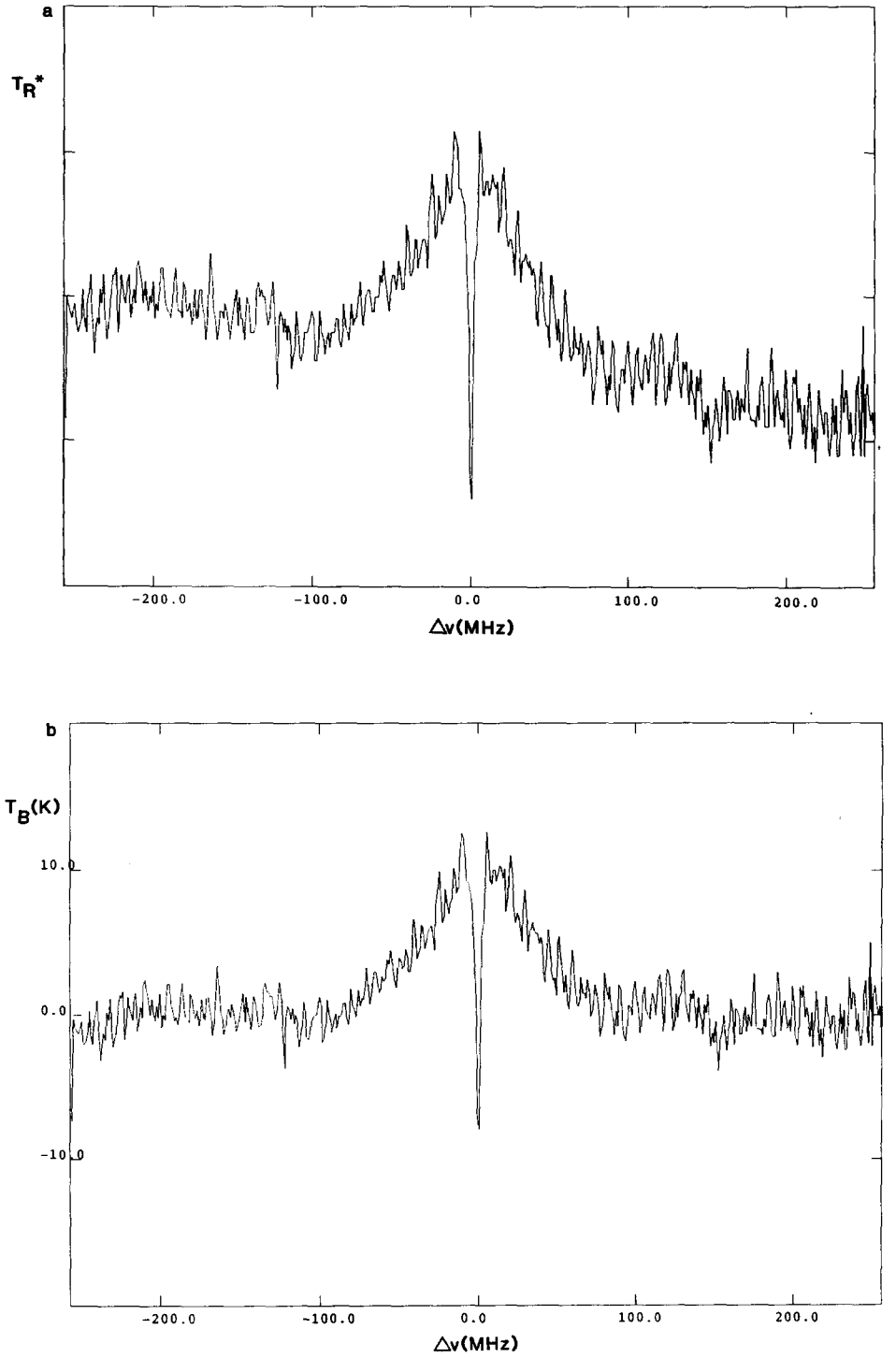

FIG. 1. Averaged observed September 1986 lines. (a) Raw ^{12}CO spectrum (arbitrary temperature scale). (b) Same after baseline removal. Resolution is 1 MHz. (c) Central part of the ^{12}CO line. Resolution is 200 kHz. (d) ^{13}CO spectrum. Resolution is 4 MHz.

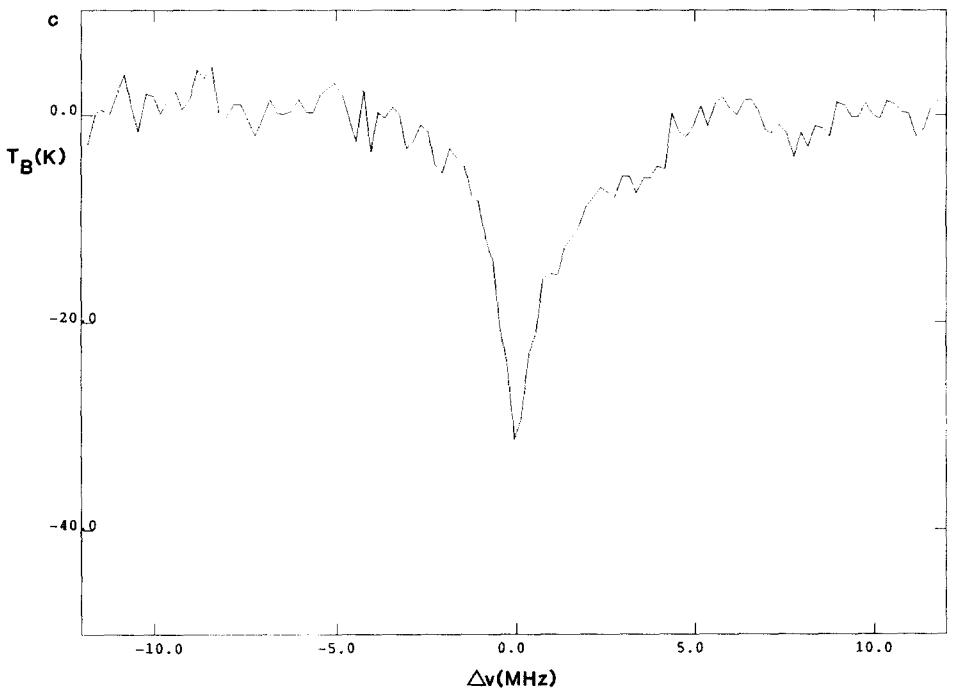

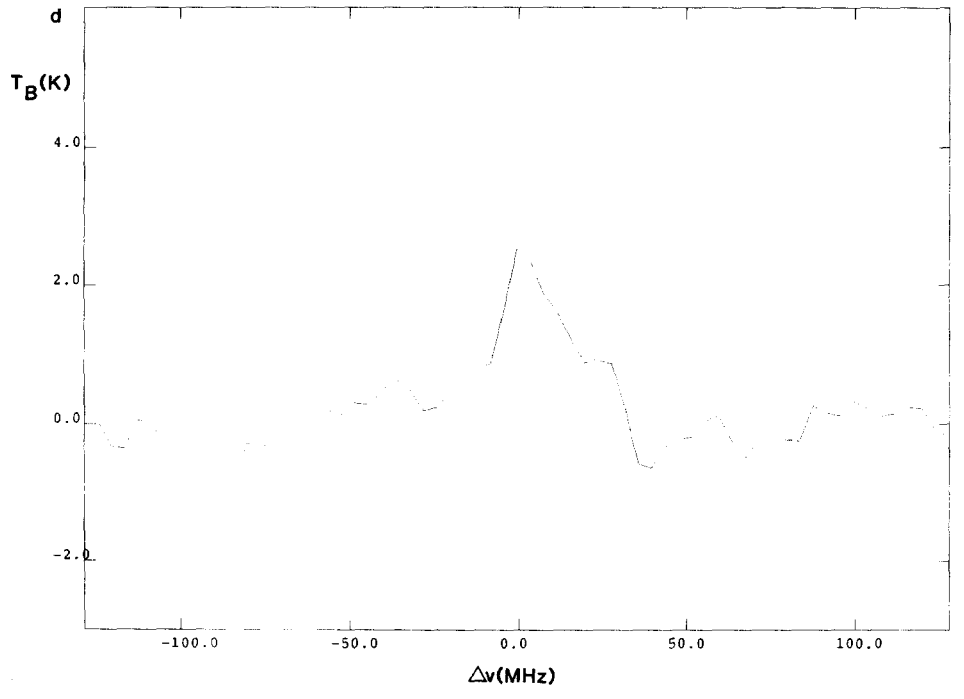

FIG. 1—*Continued.*

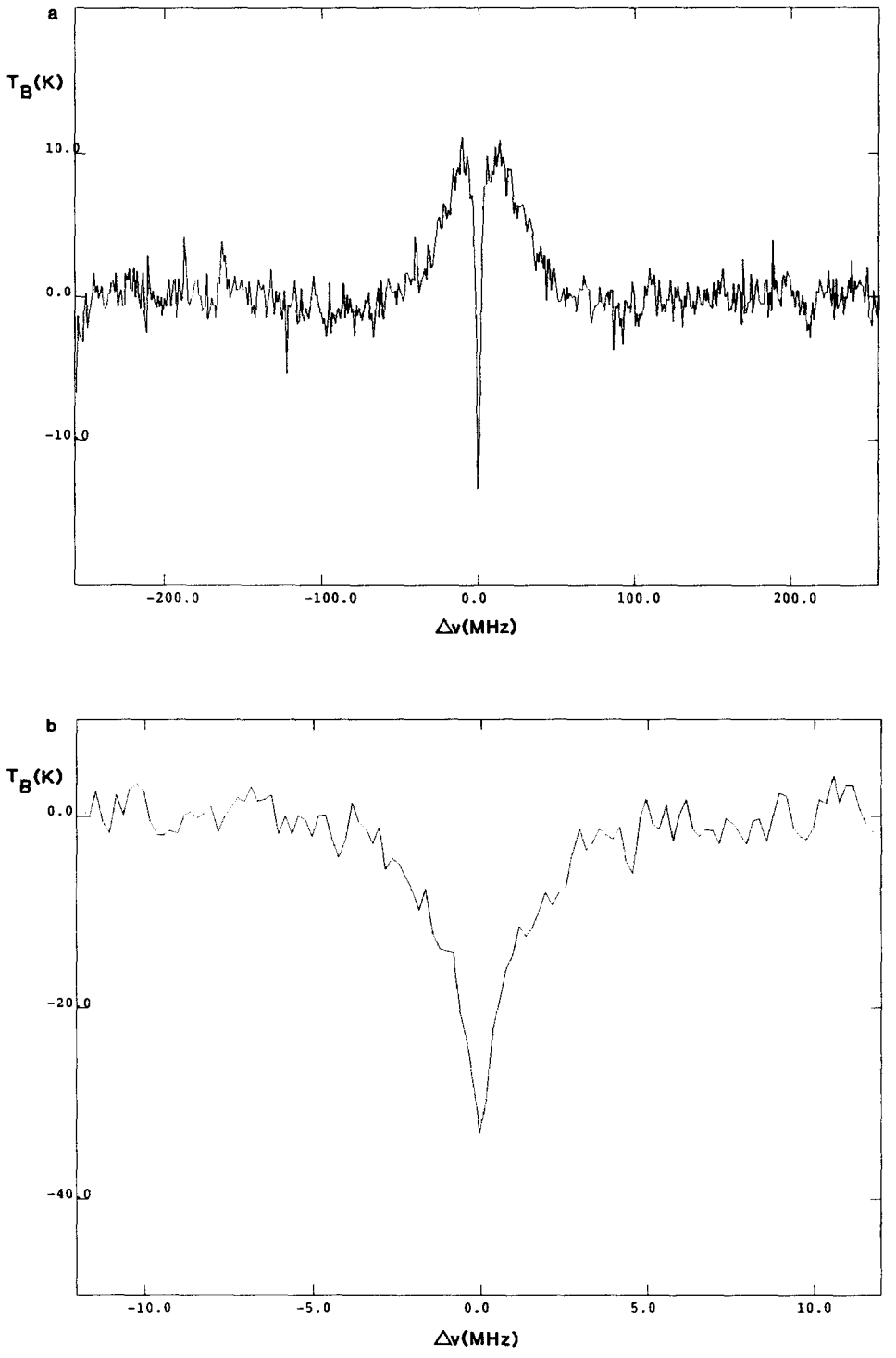

FIG. 2. Averaged observed October 1986 ^{12}CO line. (a) Overall spectrum. Resolution is 1 MHz. (b) Central part of the line at 200 kHz resolution.

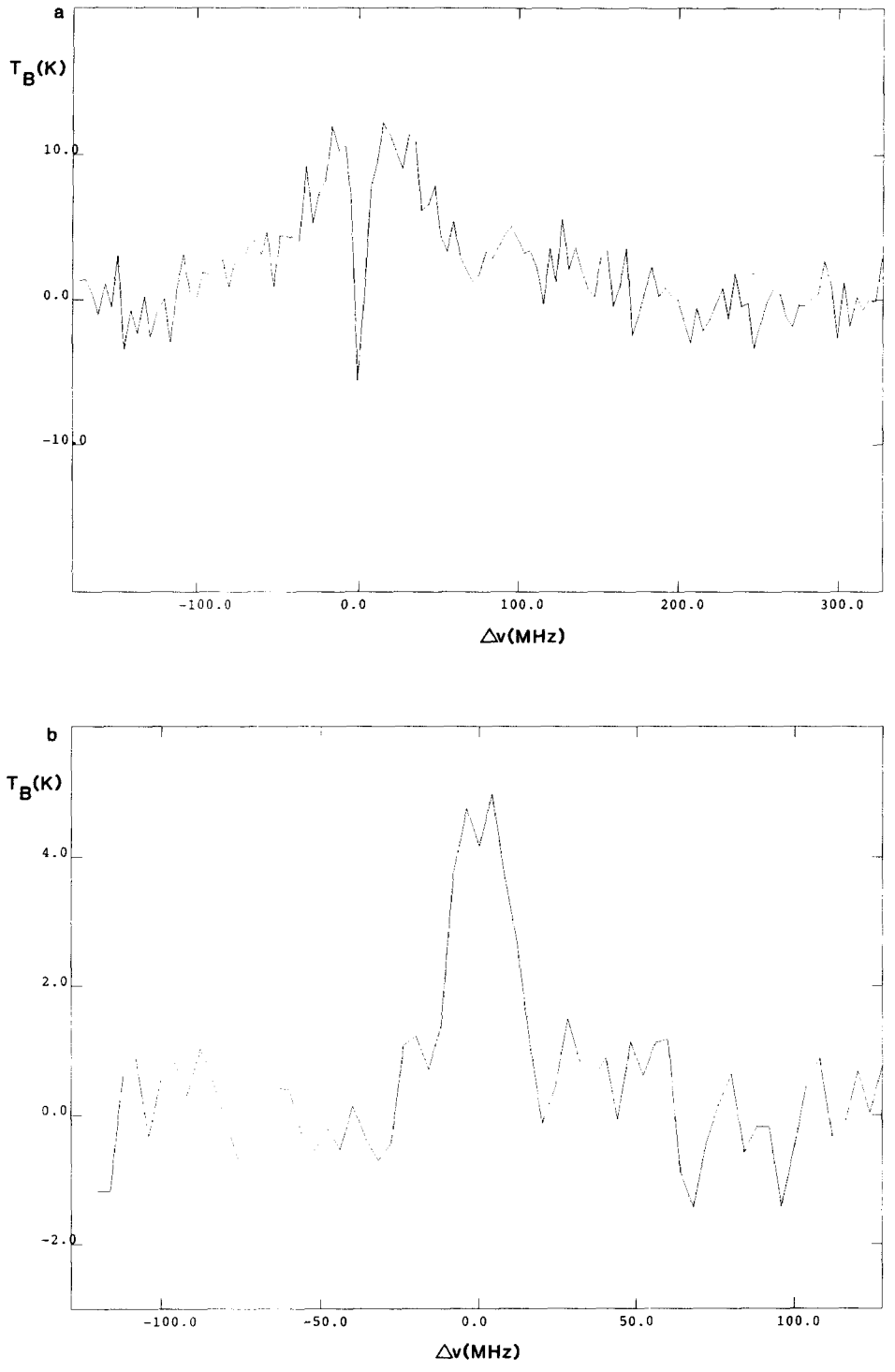

FIG. 3. Averaged observed January 1987 lines. (a) ^{12}CO line. Resolution has been downgraded to 4 MHz. (b) ^{13}CO line at 4 MHz resolution.

3. ANALYSIS

3.1. General Formulation

To analyze the data, we used a radiative transfer program which computes synthetic spectra. Observing a given position on the disk of Mars at frequency ν, the millimeter-wave brightness temperature is, in the Rayleigh–Jeans approximation

$$T_{B_\nu}(\mu) = (1 - R_P(\mu, \varepsilon))T_{surf} \exp\left(-\int k_\nu(z)dz/\mu\right) + \int k_\nu(z)T(z) \exp\left(-\int_z^\infty k_\nu(z')dz'/\mu\right)dz/\mu, \quad (1)$$

where T_{surf} is the surface temperature, μ is the cosine of the angle of incidence θ, $k_\nu(z)$ is the absorption coefficient, and $T(z)$ the atmospheric temperature at altitude z. $R_P(\mu, \varepsilon)$ is the Fresnel coefficient for reflection, which is a function of θ, of the surface dielectric constant ε, and of the polarization angle. The $(1 - R_P(\mu, \varepsilon))$ factor is then the surface emissivity for angle of incidence θ.

Since Mars is not spatially resolved in the observations, Eq. (1) must be averaged over the whole visible disk. For simplicity, we used one averaged atmospheric profile for the whole disk, and we treated Mars as a dielectric sphere with uniform surface temperature. The Fresnel coefficient was calculated as the average of the coefficients for parallel and perpendicular polarizations. ε was chosen to be 2.5 (Clancy *et al.* 1983) and the averaged surface emissivity was found to be 0.90. The absorption coefficient at a given altitude z is related to the temperature, pressure, and CO mixing ratio at altitude z (the absorption by CO_2 is negligible at 110 and 115 GHz). At the low pressures of Mars atmosphere, the Lorentz and Doppler broadening are comparable, and for modeling the lineshape we used a Voigt profile. The absolute line strengths were calculated assuming a dipole moment of 0.112 D for ^{12}CO (Kolbe *et al.* 1977) and 0.110 D for ^{13}CO (Meerts *et al.* 1977). The collisional broadening constant (CO by CO_2) was taken to be 0.11 cm^{-1}/atm at 300°K, with a $T^{-0.75}$ dependence (Varanasi 1975).

The synthetic spectrum is then a function of (i) the surface temperature T_{surf}; (ii) the averaged thermal profile $T(p)$, where the pressure p is related to z and to surface pressure via hydrostatic equilibrium; and (iii) the CO mixing ratio q.

3.2. Simple Model

3.2.1. Method. As a first step of the analysis, we assume that the temperature follows a profile similar to the one that was measured by the *Viking* spacecrafts, i.e., a linear decrease of T with z up to an altitude of about 50 km, and a constant temperature above this level (Seiff and Kirk 1977, Seiff 1982). The thermal profile is then entirely defined by the values of the surface pressure, of the temperature at 50 km (T_1), and of the temperature of the layer just above the surface (T_0). The surface pressure has been monitored by the *Viking* landers (Hess *et al.* 1980) and can be predicted as a function of the solar longitude. In this simple model, the spectrum is then a function of four parameters, T_{surf}, T_0, T_1, and q, that we assume to be constant with altitude. T_{surf} and T_0 can be different, since radiative times of the surface and of the atmosphere are different.

A preliminary study of the effect of these four parameters on the synthetical spectrum led to the following results:

As explained above, the emission wings are produced by the gas just above the surface, and the absorption core is formed in the cold upper layers. When T_{surf} is low with respect to atmospheric temperatures, the contrast between gas and surface produces large emission wings, and little or even no absorption core. As T_{surf} increases, emission wings are gradually replaced by a large absorption core. Conversely, when atmospheric temperatures are increased as a whole by a constant factor (i.e., when we shift T_0 and T_1 by identical variations, the

other parameters being fixed), the emission wings are enhanced with respect to the absorption core in the same way. A general shift in the temperatures of the atmosphere and the surface hardly affects the line profile. As may be expected, both emission and absorption are enhanced by an increase in q. Finally, the absorption is very sensitive to the atmospheric gradient (variation of T_1 only). Such a gradient has no effect on the emission far wings ($\nu - \nu_0 \geq 30$ MHz), which are formed near the surface.

It appears therefore that the ^{12}CO line profile can be used to measure three unknowns: (i) the temperature contrast between the surface and the gas just above it $\Delta T = T_0 - T_{surf}$; (ii) the temperature gradient as defined by T_1; and (iii) the ^{12}CO mixing ratio, q. The procedure used for reducing the data is then the following:

(1) The surface temperature is evaluated independently.

(2) For various values of ΔT, we first derive the q value that gives the best fit to the far wings of the line (insensitive to T_1). Then T_1 is adjusted to fit the absorption core. Finally, the rms of the residuals on the whole line is computed. The best ΔT is the one that allows minimal residuals. The corresponding T_1 and q form, together with this ΔT, our preferred solution.

(3) The derived temperature profile is then used to find the ^{13}CO mixing ratio that matches best the observed ^{13}CO line.

The surface temperature at a given point of the visible disk of Mars is a function of the epoch of the Martian year, of the location of the point on the disk (latitude and local time), and of the amount of dust suspended in the atmosphere. The averaged surface temperatures were estimated by comparing the conditions of our measurements with the ones of previous CO measurements (Kakar *et al.* 1977, Good and Schloerb 1981, Clancy *et al.* 1983). In all our observations, the subearth point was close to the equator, which rules out most seasonal effects. A factor of uncertainty on this temperature is the amount of dust at the time of the observations. As we said, observations were made near perihelion (25 September 1986), a period when large amounts of dust are usually present in the atmosphere. Nevertheless, Pollack *et al.* (1979) predicted that the diurnally averaged temperature of the surface would not be seriously affected by an even large amount of dust, and that the diurnal temperature amplitude of the surface would slowly decrease with increasing dust optical depths. Therefore, the surface temperature should not be affected by more than a few degrees Kelvin by the dust. In any case, as shown above, this uncertainty on the surface temperature shows practically no influence on the determination of the other parameters.

3.2.2. Results. Results of the three-parameter fit of the ^{12}CO line are presented in Table II. Best fits are shown in Figs. 4 to 6. The quoted error bars were obtained as follows:

(*a*) *Errors due to the procedure.* As is clear from the sequential fitting procedure, errors on the derivation of ΔT influence the estimation of the other two parameters. Therefore, for a number of various ΔT's, we calculated the residuals for a grid of points (T_1, q) in order to find the domain where the residuals do not exceed the rms obtained for the preferred solution by more than 1 SD (this was our criterion for deriving the error bars). For each ΔT, a domain of possible (T_1, q) was thus found. The range of admissible ΔT was obtained by saying that, for the extreme possible ΔT, the best fit fulfills the 1 SD criterion. Finally, this gave us the box of possible ΔT, T_1, q, assuming the calibration is perfect.

(*b*) *Errors due to the calibration.* As we said before, we believe the calibration is accurate to $\pm 15\%$. To evaluate the effect of this uncertainty, we calculated the best solutions for lines obtained by multiplying channel by channel the September 1986 line by factors 1.15 and 0.85, respectively. We found that the corresponding parameters we derived did not differ from those ob-

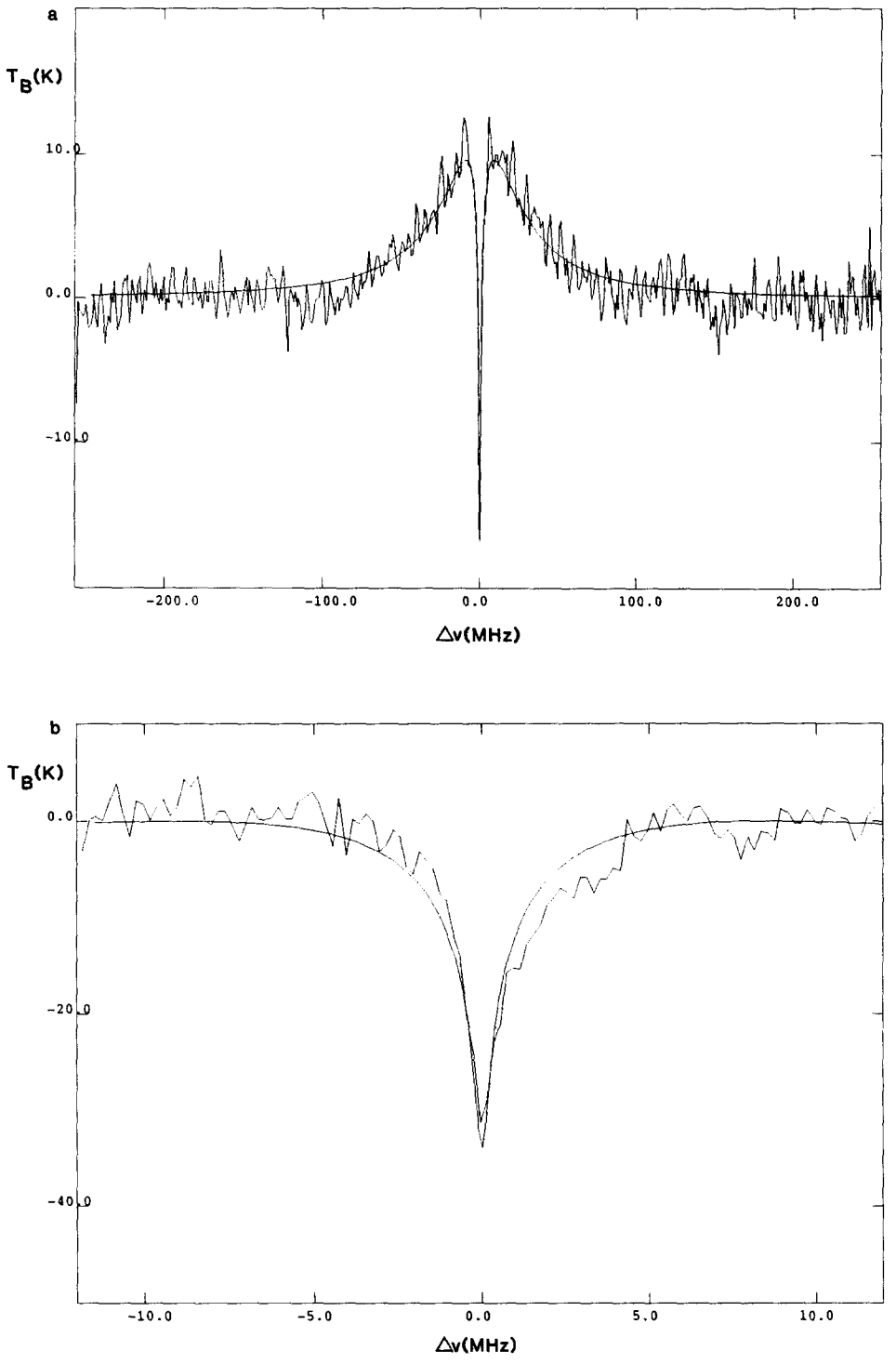

FIG. 4. (a,b) Best fit of the September ^{12}CO line in the "linear atmosphere" model. Corresponding atmospheric temperatures and CO mixing ratio are given in Table II.

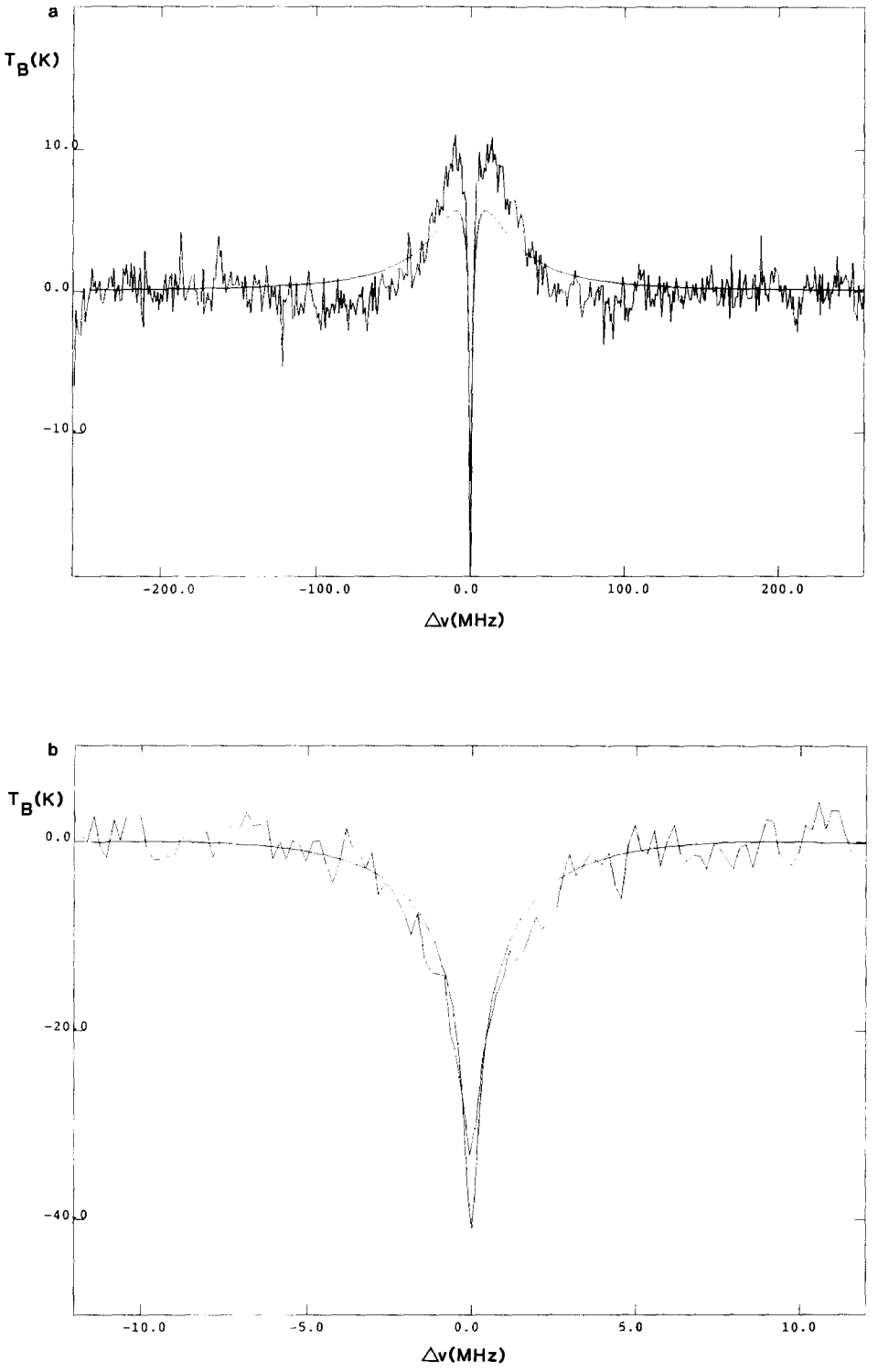

FIG. 5. (a,b) Same as Fig. 4 for October line.

TABLE II

REDUCTION OF THE OBSERVATIONS IN THE "LINEAR" MODEL

Observation	September 1986	October 1986	January 1987
Predicted surface pressure (mbar)	8.8	8.8	8.3
Estimated surface temperature (°K)	230	220	225
Model derived parameters			
Contrast gas-surface (°K)	+18 +25/−16	+20[a]	+5 +20/−10
Temperature at 50 km (°K)	170 +12/−18	133[a]	186 +12/−22
^{12}CO mixing ratio	3.3 +1/−1.5 × 10^{-4}	1.7×10^{-4}	7 +1.5/−3 × 10^{-4}
$^{12}CO/^{13}CO$	13 +40/−8	—	13 +50/−8

[a] See text.

tained in the case of the "nominal" September line by more than about 25% of the size of the above described box. That is, the uncertainty due to the calibration is much less important than the one introduced by the fitting procedure. Because of this result, we obtained the final error bars by simply convolving the two factors of uncertainty.

For October 1986 data, no uncertainty estimation was performed. Indeed, as shown in Fig. 5, the preferred solution gives a very poor fit and an error analysis would not make any sense. We conclude that, unlike September and January data, which can be reasonably well fitted with a simple, *Viking*-type linear temperature

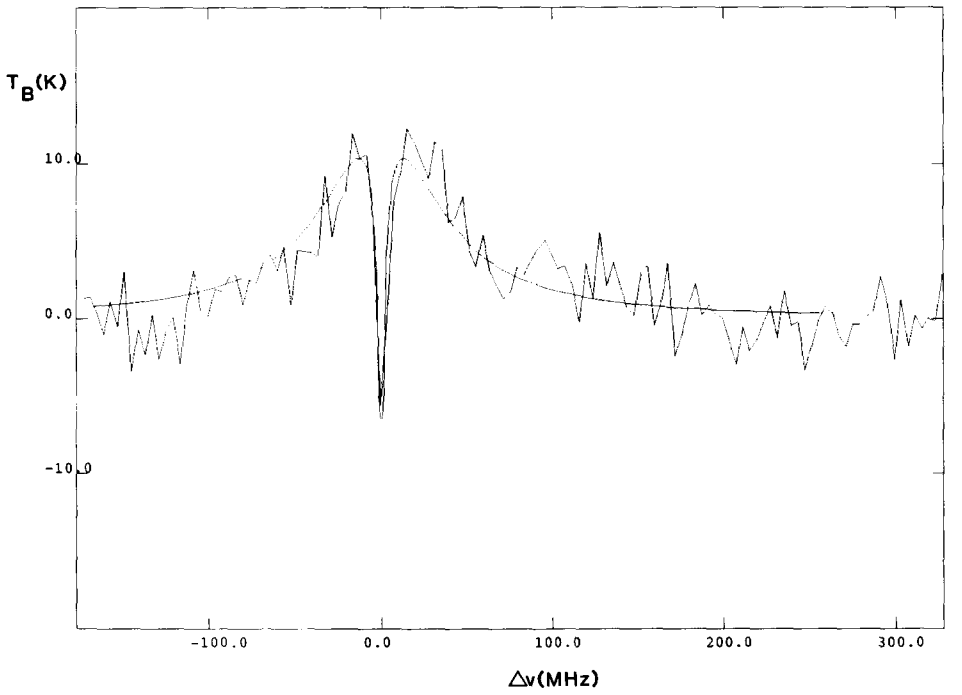

FIG. 6. Same as Fig. 4 for January line.

model, October data imply a significant change in the thermal profile structure. Of course, a satisfactory profile is still to be found.

Results concerning the ^{13}CO line are presented in Fig. 7 and Table II. For the error analysis, we calculated best fits of the line with the whole range of linear thermal profiles allowed by the ^{12}CO lines. ^{13}CO mixing ratios leading to 1 SD were evaluated in each case. The uncertainty due to calibration was included as for ^{12}CO lines. This finally provided a range of allowed ^{13}CO mixing ratios. From this and the range of allowed ^{12}CO mixing ratios, the range of possible $^{12}CO/^{13}CO$ is obtained for September and January observations. Actually, the possible range for the isotope ratio is smaller than indicated, because, for example, it is certainly not possible to have at the same time the maximal ^{12}CO abundance and the minimal ^{13}CO abundance (no linear thermal profile would allow one to fit both of the lines at the same time). It must be pointed out that September and January observations agree with a $^{12}CO/^{13}CO$ equal to 13 +45/−8, the error bars here being probably overestimated. This gives us the second conclusion: if the thermal profile varies linearly with altitude, the September and January data give a value of the $^{12}CO/^{13}CO$ ratio which is definitely not compatible with the terrestrial value of the $^{12}C/^{13}C$ isotopic ratio (89). Because such a result is puzzling (see further a discussion of possible mechanisms to enrich ^{13}CO), the next step is to see whether the observed lines can be explained with a terrestrial $^{12}CO/^{13}CO$ and a realistic thermal profile.

3.3. Inversion of the Temperature Profile

3.3.1. Method. In this section, we will invert the observed ^{12}CO lines; i.e., assuming a given value of the CO mixing ratio, we will infer the atmospheric thermal profile necessary to explain the lines. As explained above, the spectra are very sensitive to the surface temperature, but only through the contrast surface/first atmospheric layer. Therefore, we have to use surface temperature as an input parameter to measure atmospheric temperatures.

We use a standard inversion method based on concepts developed by Chahine (1968). A number of frequencies are selected which cover the whole line. Each frequency i is associated with an atmospheric level z_i, taken near the peak of the weighting function at frequency i. Starting with a given set of temperatures T_i, a complete profile is obtained by linear interpolation, and a synthetic spectrum is calculated. Because of the surface contribution and because the data give only the contrast line/continuum, the iteration algorithm has to be slightly modified. We use

$$T_i^{n+1} = T_i^n \times \left(\frac{T_{\text{exp}} - C_s^n}{C_{\text{atm}}^n}\right)_i,$$

where the atmospheric contribution is equal to

$$C_{\text{atm}}^n = \int \mu d\mu \int T^n(z) d\left[\exp\left(-\int_{z_i}^{\infty} k_i(z')dz'/\mu\right)\right]$$

and the surface contribution is

$$C_s^n = \int \mu d\mu T_{\text{surf}}(1 - R_P(\mu, \varepsilon)) \times \left[\exp\left(-\int_0^{\infty} k_i(z')dz'/\mu\right) - 1\right].$$

Iteration is performed until the calculated and observed spectra differ by less than the noise in the observed spectrum. We chose the following frequencies (measured in MHz) from the center of the line: 80, 25, 10, 4, 1.8, 0.8, 0.3, and 0. Figure 8 shows the weighting functions, calculated for a CO mixing ratio equal to 10^{-3}. The corresponding z_i depend on the mixing ratio, but are always more or less equally spaced between 0 and 65–75 km. As a starting profile, we always assume an isothermal atmosphere at 200°K. This method was tested successfully on various synthetical spectra. Figure 9 shows the application to the September 1986 ^{12}CO line, assuming a CO mixing ratio of 3.3×10^{-4}, the value derived in

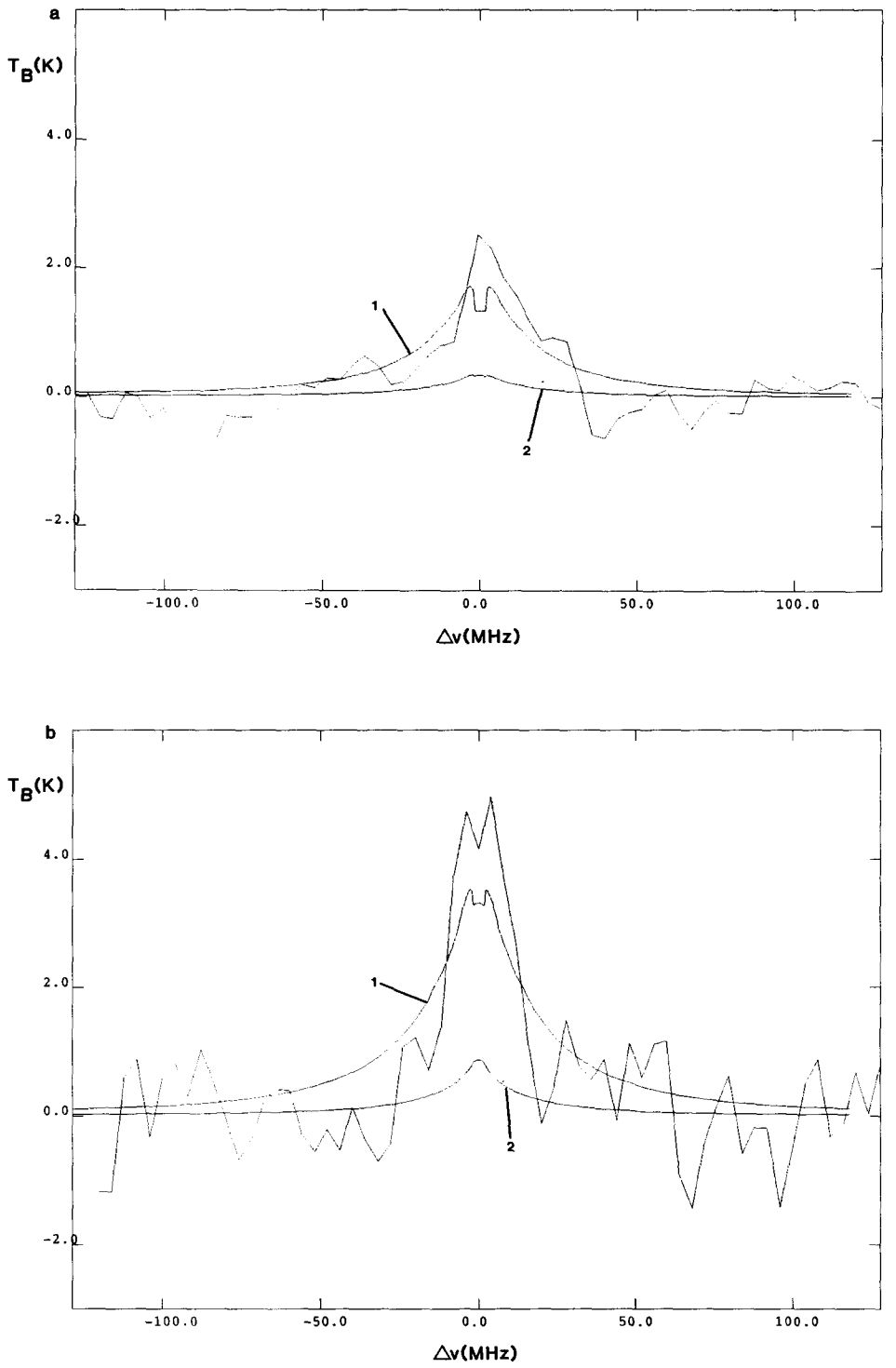

FIG. 7. Best fit of the (a) September and (b) January ^{13}CO lines. Synthetical spectra are calculated for $^{12}CO/^{13}CO$ ratios of 13 (curve 1, best fit) and 89 (curve 2).

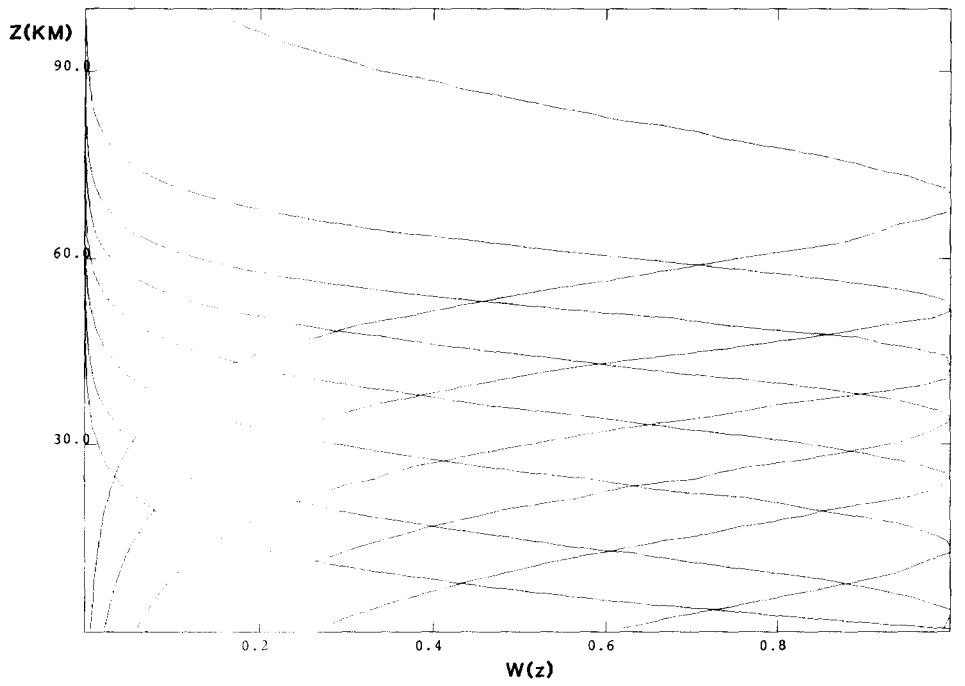

FIG. 8. Weighting functions for a CO mixing ratio equal to 10^{-3}. Frequencies are (from top to bottom): 0, 0.3, 0.8, 1.8, 4, 10, 25, and 80 MHz from the center of the line.

the linear model. The result is satisfactory: the profile is quasi-linear under 50 km and a tendency to isothermality appears above 50 km. In the lower part ($z \leq 20$ km), the retrieved model deviates somewhat from the linear model. This is consistent with the fact that the fit is improved in the wings of the line.

3.3.2. Results. We first inverted the September line for various CO mixing ratios. For each resulting profile, synthetical ^{12}CO and ^{13}CO lines were recomputed, assuming $^{12}CO/^{13}CO = 89$, and compared to data. Figure 10 shows three of these profiles. It can be seen that the more the assumed mixing ratio q is different from the linear model value, the more dramatic the thermal profile is. In particular, for large values of q, the obtained 0-km atmospheric temperature becomes much lower that the surface temperature and a strong positive temperature gradient develops in the first 10 km. On the other hand, large values of q are necessary to reproduce the ^{13}CO line. We find that the best-fit compromise of the two lines is obtained when $q = 2 \times 10^{-3}$. The profile is one of those shown in Fig. 10 and the corresponding lines are shown in Fig. 11.

The same approach was used for the January lines. In this case, however, due to the poor quality of the ^{12}CO line, the resolution had to be downgraded to 4 MHz, and little information is available on the shape of the absorption line. Therefore, we had to limit the retrieval of the thermal profile to the 0–20 km region. Qualitatively, the same conclusions hold as for September spectra. The best compromise is obtained for $q = 4 \times 10^{-3}$ and is shown in Fig. 12.

We finally inverted the October 1986 line, using the same method. The spectrum can be fitted within quite a large range of CO values. Figure 13 shows the result for $q = 2 \times 10^{-3}$. In the absence of any ^{13}CO line, as for September and January, it is not possible to further constrain the abundance of

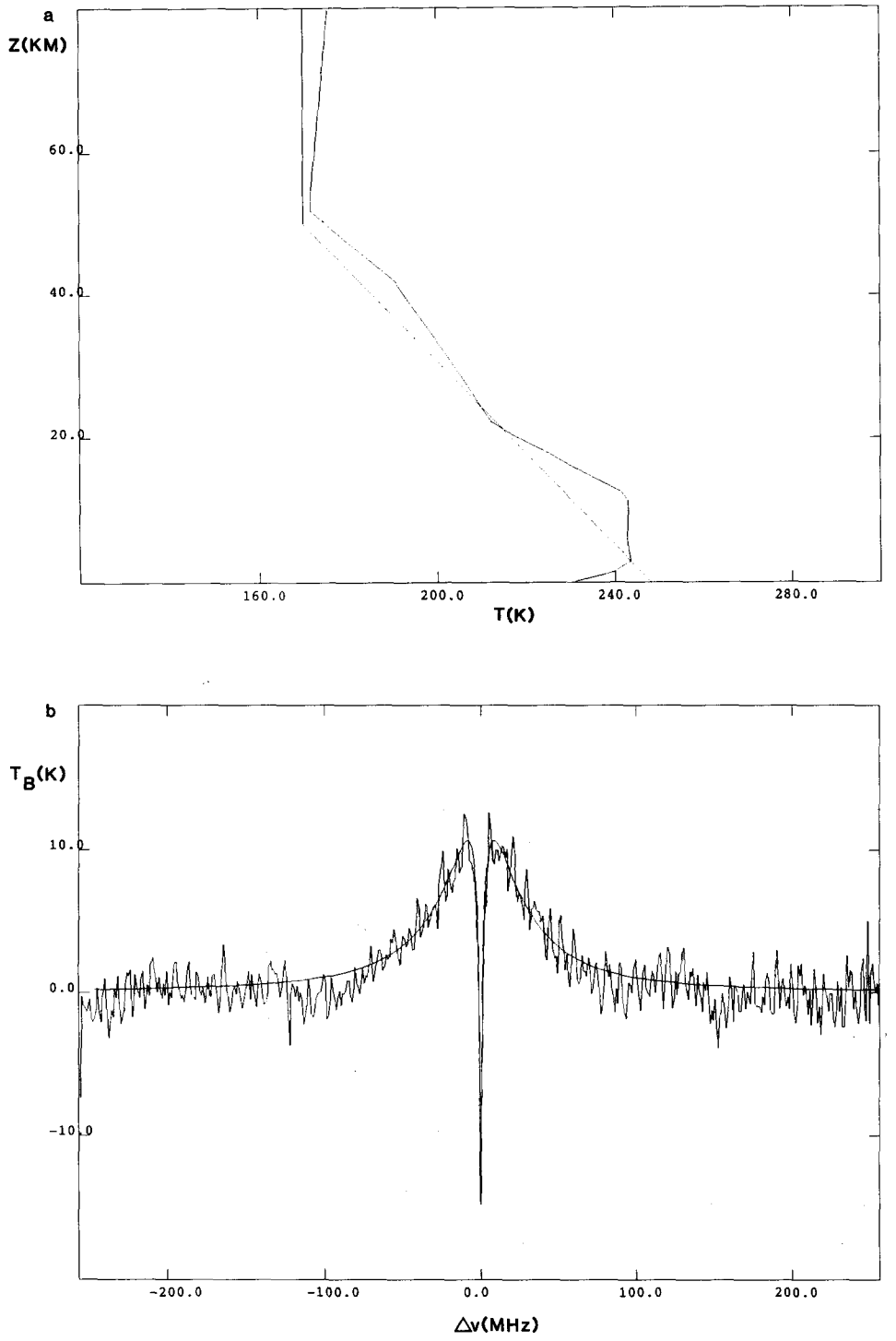

FIG. 9. Inversion of the ^{12}CO September 1986 line for a CO mixing ratio equal to 3.3×10^{-4}. (a) Comparison of the retrieved profile with the atmosphere obtained in the "linear model." (b) Fit of the line with the retrieved profile.

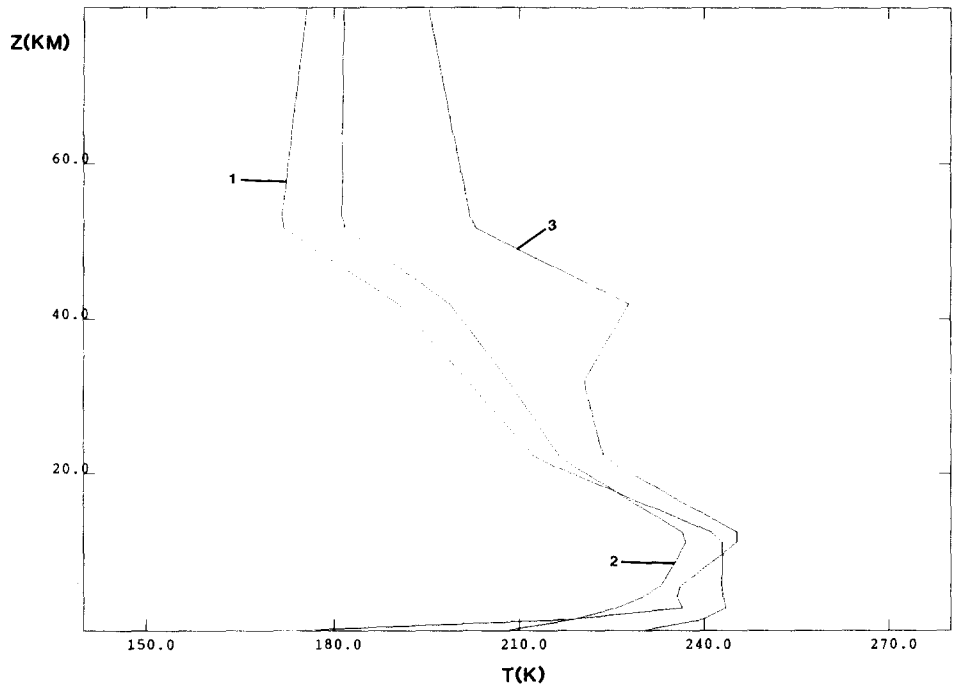

FIG. 10. Retrieved profiles from the ^{12}CO September line for various CO mixing ratios: (1) 3.3×10^{-4}, (2) 5×10^{-4}, (3) 2×10^{-3}.

CO. We note, however, that whatever the CO mixing ratio is, the retrieved profile shows a strong positive temperature gradient in the first 10 km. Note also that the negative temperature gradient between 10 and 50 km is always moderate, compared to *Viking* profiles (typically 1°K/km vs 1.4°K/km for *Viking* profiles). This is also true with the profiles retrieved from the September data.

4. DISCUSSION

Our millimeter-wave observations lead to the following conclusions:

(a) The September 1986 and January 1987 lines can be fitted reasonably well with the assumption of a temperature profile showing a simple linear dependence on altitude, quite similar in shape to those recorded by the *Vikings*. The measured CO abundance is then relatively low and varies from September to January by a factor of about 2.5 (3.3×10^{-4} to 7.5×10^{-4}). In this case, however, the observed ^{13}CO lines suggest a strong ^{13}CO enrichment (factor 2 to 15) and are definitely not compatible with a terrestrial $^{12}C/^{13}C$.

(b) If the $^{12}CO/^{13}CO$ is constrained to be equal to the terrestrial value of 89, inversion of the lines leads to quite higher values of CO mixing ratios, and to an increase of this mixing ratio by a factor 2 between September and January (2×10^{-3} to 4×10^{-3}). In this case, the retrieved thermal profiles exhibit a very cold atmospheric temperature (170–180°K) near the surface and strong temperature gradients in the first 10 km.

(c) The October data cannot be reproduced with the assumption of a linear profile. Whatever the CO abundance is, they imply the same kind of thermal structure with a strong positive gradient from a very

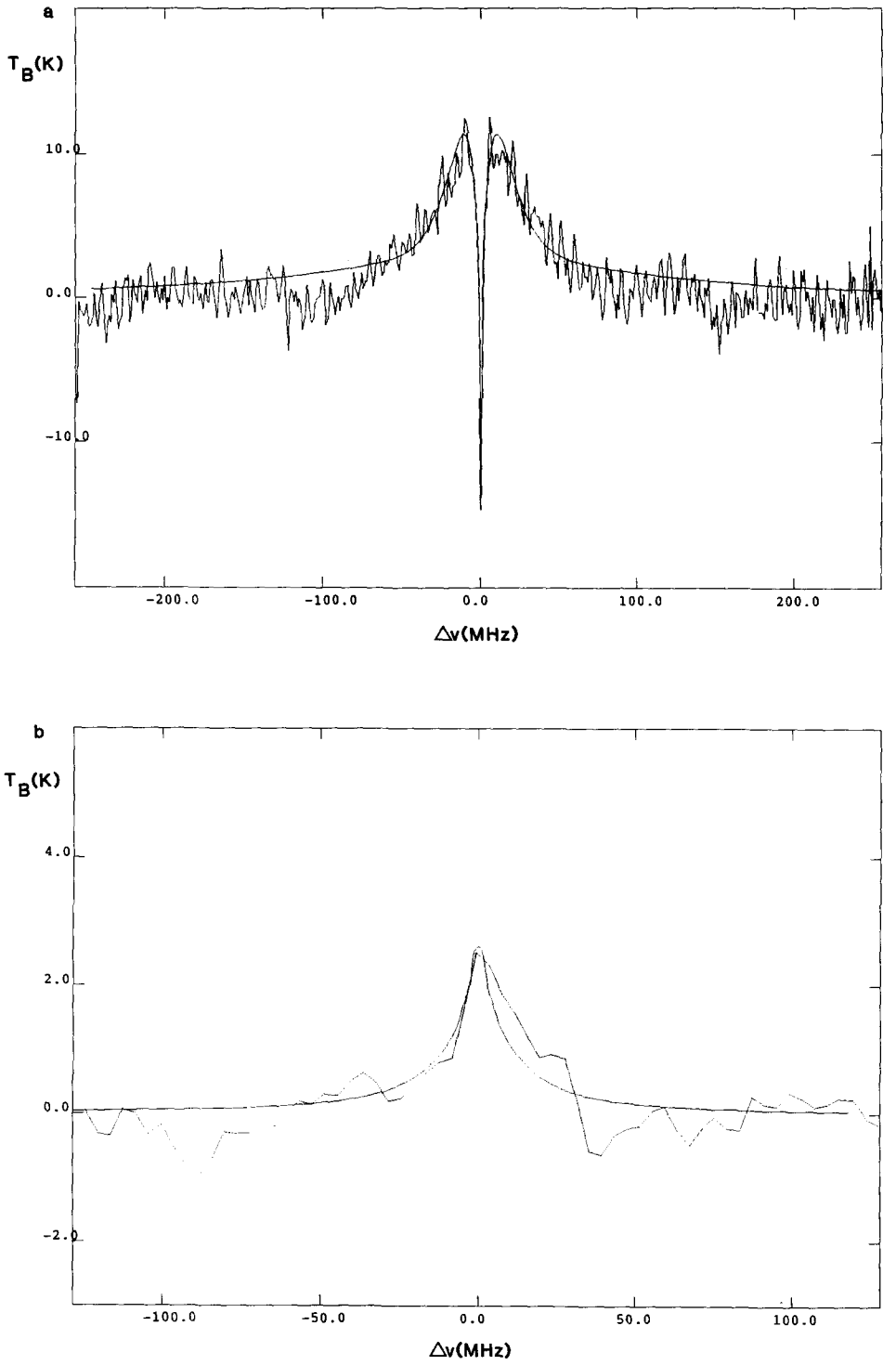

FIG. 11. Fit of the September lines with the retrieved profile for $^{12}CO = 2 \times 10^{-3}$. (a) ^{12}CO line. (b) ^{13}CO line. The isotope ratio is 89.

cold gas temperature at the surface. No real constraint can be put on the CO abundance.

Thus, the entire set of data gives indications of a few possible "anomalies". A firm conclusion is that the thermal profile in October 1986 was "abnormal" (i.e., quite different from a *Viking*-type profile). September and January data can also be explained in terms of "abnormal" thermal profiles and terrestrial CO isotope ratio. All three spectra were taken at solar longitudes (240°–320°) corresponding to periods of generally large dust activity, which could account for a modification of the thermal profile.

As we said, both the linear model and the inversion of the September and January data assuming an isotope ratio of 89 lead to an increase of CO by a factor 2 in 4 months, which is at first glance puzzling when compared to the variation time predicted by Hunten (1974; 2 years). We cannot demonstrate that CO has varied by a factor 2 between September and January, because it would be quite possible to invert both sets of data with a constant mixing ratio (for example, 7.5×10^{-4}, which would have the advantage of allowing one to retrieve a more or less linear profile for January), but then at least one of the two data sets would not be compatible with a terrestrial isotope ratio.

Therefore, it looks reasonable not to reject a priori any of the possibilities. We first discuss the possibility of an anomalous isotope ratio, and then the thermal profile and CO abundance short-term variability.

(1) The $^{12}CO/^{13}CO$ ratio. As we said before, the only direct observation of ^{13}CO in Mars atmosphere prior to our measurement is due to Kaplan *et al.* (1969). Their analysis of the ^{12}CO and ^{13}CO lines at 1.6 μm showed compatibility with a $^{12}CO/^{13}CO$ ratio of 100. Determinations of the Martian $^{12}C/^{13}C$ from CO_2 measurements agree with the terrestrial value: heterodyne 10-μm observations of $^{12}CO_2$ and $^{13}CO_2$ lines (Schrey *et al.* 1986) indicate a Martian $^{12}C/^{13}C$ of 96 $\pm$ 6, in complete agreement with the value measured by the mass spectrometer aboard the *Viking* probes (90).

Still, CO not being the main C-bearing constituent of Mars atmosphere, the $^{12}CO/^{13}CO$ ratio can in principle be different from the $^{12}C/^{13}C$, measured by $^{12}CO_2/^{13}CO_2$. In this case, a mechanism must be found that could allow for the enrichment of ^{13}CO with respect to $^{13}CO_2$.

Fractionation effects are known to occur in the interstellar medium (Combes *et al.* 1980). However, the mechanism that is proposed (reaction between C^+ and CO) is efficient only at $T \leq 35$°K (Watson *et al.* 1976) and is therefore irrelevant here.

As noted by Clancy and Muhleman (1983), the equilibrium partitioning of ^{13}C between CO and CO_2 (reaction $^{12}CO + {}^{13}CO_2 \rightleftarrows {}^{13}CO + {}^{12}CO_2$) always leads to ^{13}CO depletion.

Gravitational separation cannot be invoked as well, since the ^{13}CO abundance we measure refers to layers close to the surface, where the components are uniformly mixed.

A possible explanation might lie in different photodissociation rates of $^{12}CO_2$ and $^{13}CO_2$. In the case of the Earth's atmosphere, the enhancement of heavy ozone is interpreted by a higher dissociation rate for $^{18}O^{16}O$ than for $^{16}O^{16}O$. A higher photodissociation rate of heavy $^{13}CO_2$ would be responsible for a higher production of ^{13}CO on the dayside of the planet. A difference in transport efficiency between ^{12}CO and ^{13}CO would lead to a better redistribution of lighter ^{12}CO on the nightside of the planet. Combination of the two processes would lead to an enrichment of ^{13}CO on the observed (morning) side of Mars. Another possibility might lie in different recombination rates of ^{13}CO and ^{12}CO with OH (see next section). Yet, these suggestions remain qualitative, and they could only partially account for the measured 2- to 15-fold enrichment. Therefore, we believe the hypothesis of an anomalous isotope ratio is difficult to support and warrants examina-

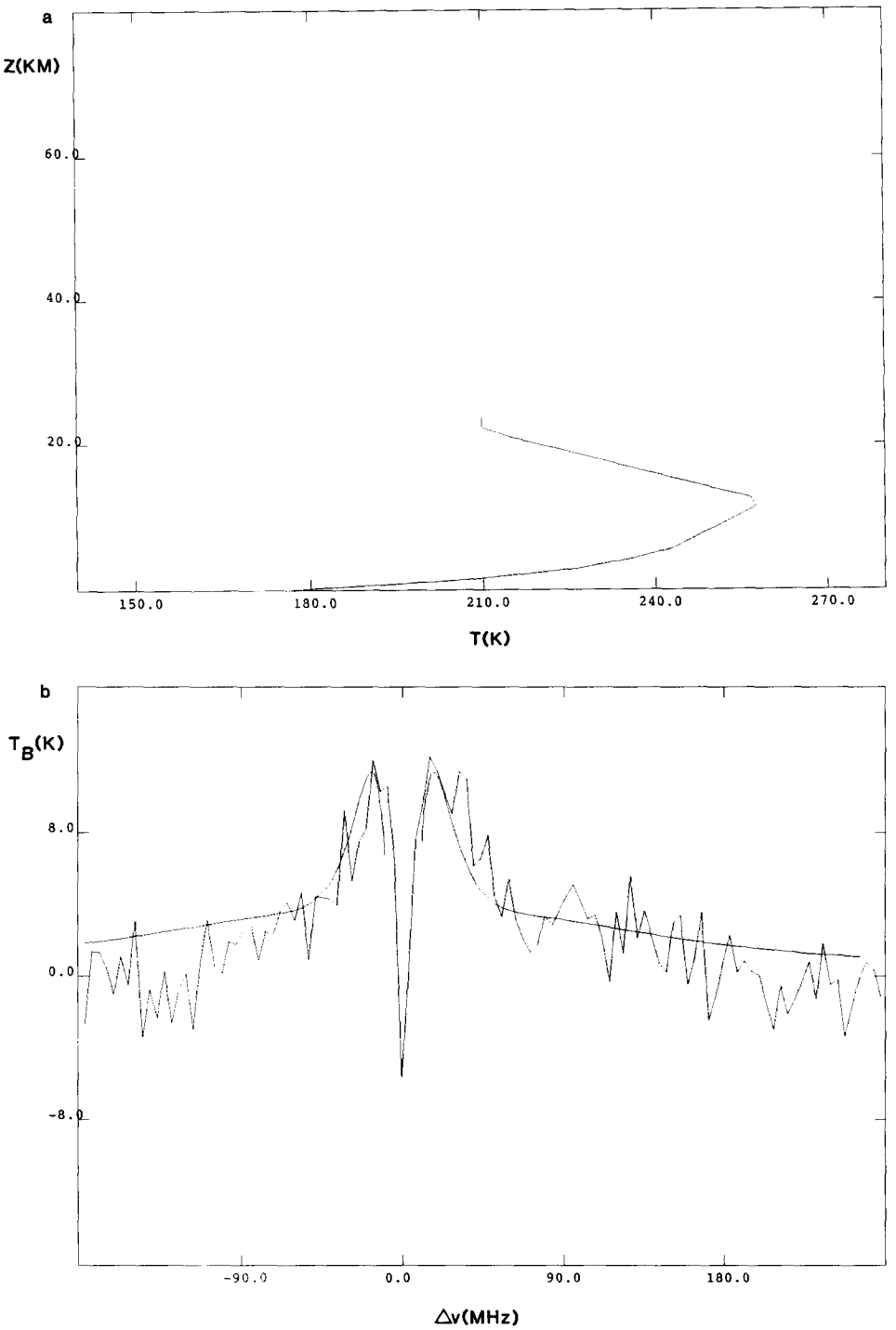

FIG. 12. Inversion of the January lines for $^{12}CO = 4 \times 10^{-3}$ and $^{12}CO/^{13}CO = 89$. (a) Retrieved profile (below 20 km only). (b) ^{12}CO line. It has not been attempted to fit the center of the line. (c) ^{13}CO line.

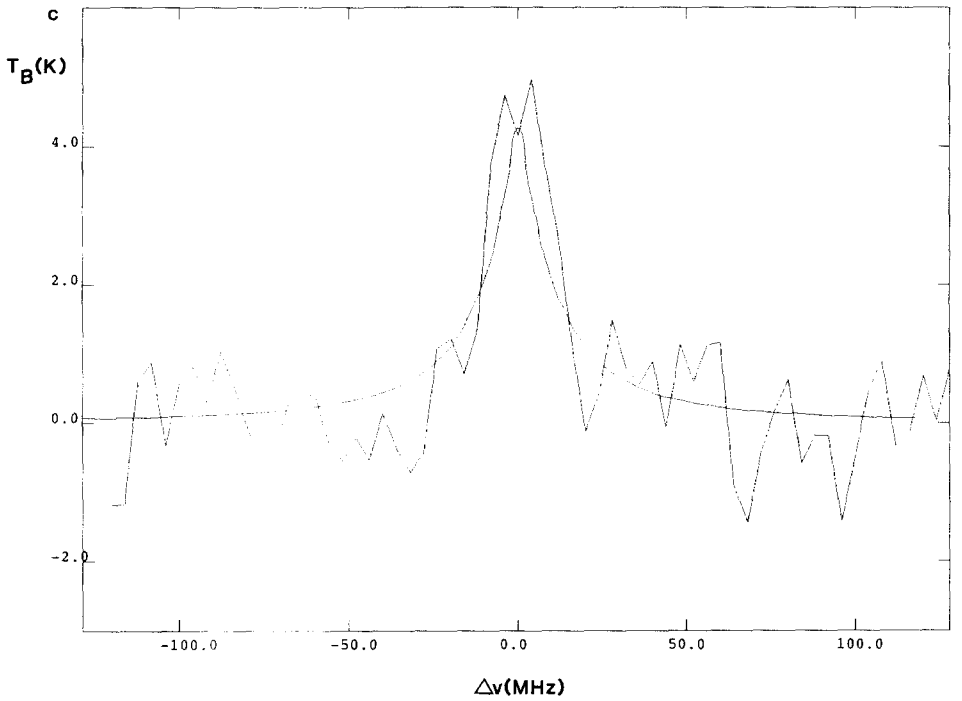

FIG. 12—*Continued.*

tion of other possibilities, e.g., an "abnormal" thermal profile and short-term CO variability.

(2) *The thermal profile.* Pollack *et al.* (1979) have extensively studied the properties and effects of dust particles in the Martian atmosphere. They predicted that the (diurnally averaged) surface temperature, as well as the temperature of the lowest atmospheric layers, is almost not affected by the dust, whereas the relatively cold upper atmospheric layers are noticeably warmed by the dust. This tends to isothermalize the atmosphere.

Our October observation implies a significant modification of the thermal structure with respect to "dust-free" conditions, especially in the first 10 km. The most striking features are probably the very cold gas temperature near the surface and the very strong temperature gradient in the first 10 km. In the assumption of a terrestrial $^{12}CO/^{13}CO$, the September and January thermal profiles show the same qualitative behavior. Between 10 and 50 km, we observe, for September and October profiles, that the average negative gradient is significantly lower than in the cases of the Viking profiles (1 vs 1.4°K/km), in agreement with Pollack *et al.* (1979). Warming of the upper atmosphere and cooling of the lower can be qualitatively understood in terms of dust opacity. Solar radiation is absorbed by the dust in the upper atmosphere, which warms up the atmosphere. Dust opacity becomes large in the lower layers, which prevents radiation to penetrate and to heat the gas. However, in the absence of firm quantitative independent information of the dust state of the atmosphere at the time of our measurements, it is not possible to go further in the discussion.

(3) *The variability of CO abundance in the Mars atmosphere.* Temporal variability

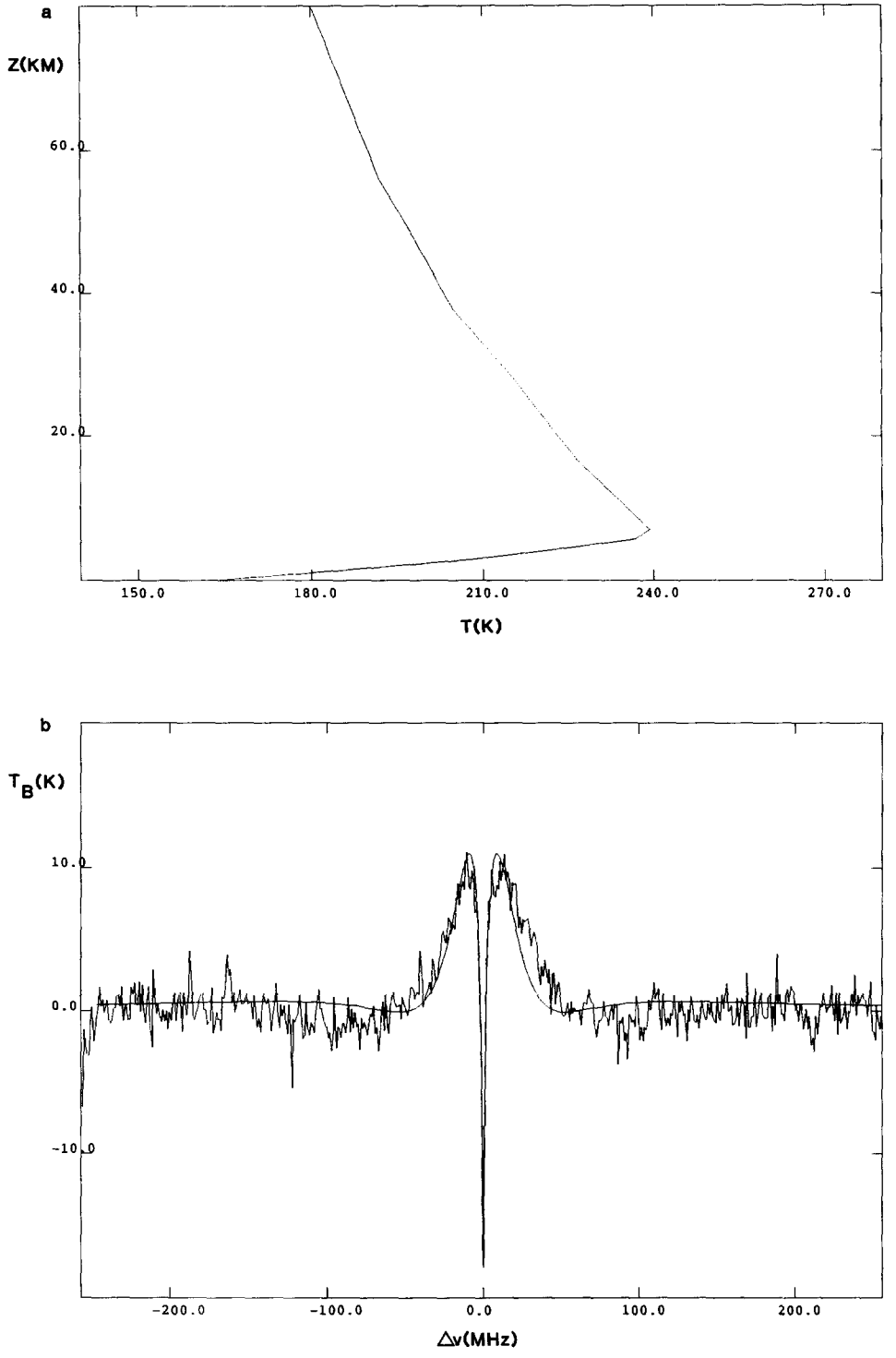

FIG. 13. (a,b) Inversion of the October line for CO = 2×10^{-3}. Retrieved profile and corresponding line.

of CO in the Mars atmosphere has been studied for one decade. Good and Schloerb (1981) were the first to point out observational evidence of temporal variations in the CO abundance, from a comparison of their observation of the $J = 1–0$ line with Kaplan *et al.*'s (1969) measurement. They concluded that a fourfold increase in the CO abundance occurred over 15 years. On the other hand, a careful reanalysis of all millimeter-wave observations up to 1982 led Clancy *et al.* (1983) to the conclusion that the data allowed for a range of CO variability from 0 to 100%, i.e., that a temporal variability, although not excluded, could not be definitely established. However, all determinations of CO are based on an assumption of the thermal profile (e.g., our September 1986 line can be fitted with CO abundances differing by almost an order of magnitude) and an unambiguous measurement of CO requires simultaneous observations of at least two CO lines. If the $^{12}CO/^{13}CO$ mixing ratio is assumed to be 89, a ^{13}CO line can be used. Using this method, we derive for September and January observations CO mixing ratios of 2×10^{-3} and 4×10^{-3}, respectively. Our purpose here is not to compare these values with previous CO measurements, but to discuss the plausibility of a variation by a factor of 2 in 4 months.

CO is produced in the atmosphere of Mars from the photodissociation of CO_2, i.e.,

$$CO_2 + h\nu \rightarrow CO + O \qquad (R1)$$

Atomic oxygen, in turn, recombines to form O_2. Recycling of CO_2 by the reverse reaction (R1) is spin forbidden, so that in the absence of any other recycling mechanism, all the Martian CO_2 would be irreversibly destroyed by photolysis in about 10^4 years. However, CO_2 is observed to be stable and shows only seasonal variations, and CO and O_2 do not build up beyond approximately 0.1% of CO_2. The most likely accepted mechanism to regenerate CO_2 is

$$CO + OH \rightarrow CO_2 + H \qquad (R2)$$

OH is produced from the photolysis of H_2O, as well as from the reaction of $O(^1D)$ with H_2O, and from the photolysis and reaction of HO_2 with H. The abundance of water vapor is constrained by the saturation law. Reaction (R2) is more effective below 40 km, where H_2O is more abundant, and efficient downward transport of CO from its production altitude is needed. An eddy mixing coefficient of 10^8 cm^2 sec^{-1} or greater at the homopause is required (Mc Elroy and Donahue 1972, Liu and Donahue 1976).

From this scheme, it is clear that the abundance of CO is controlled largely by the abundance of water and the atmospheric mixing. H_2O exhibits seasonal variations. Its abundance has been measured to range from 2 to 60 precipitable microns. In addition, during periods of dust storms, the atmospheric H_2O can vary dramatically, and so can the mixing which transports the CO to the region below 40 km. Changes in the surface and atmospheric temperatures play an important role in determining the limiting vapor pressure of H_2O and hence the OH abundance. On a globally and seasonally averaged basis, large changes in the CO mixing ratio are not expected as CO produced from CO_2 has a time constant of approximately 3 years (Mc Elroy *et al.* 1977). During periods of dust storms and other sporadic or irregular phenomena, however, changes in CO abundances can be expected due to changes in atmospheric/surface temperatures, water vapor amounts, and the atmospheric vertical mixing. These changes could be global or local. From reaction (R2), an anticorrelation is expected between CO and H_2O. In view of the many factors that could affect OH as well as CO downward flux, a change in the CO abundance by a factor of 2, as observed in this study, does not seem unrealistic. An ideal observation to test this hypothesis would involve simultaneous measurements of CO, H_2O, and O_2, and of the dust opacity.

Finally, we believe, in spite of some un-

expected results, that the most plausible explanation of our entire set of observations is that the $^{12}CO/^{13}CO$ is terrestrial, and that there are strong indications of temporal variations in the thermal profile and the CO abundance. It would be a useful experiment to observe two ^{12}CO lines and one ^{13}CO line simultaneously to help alleviate the ambiguity in the analysis.

5. CONCLUSION

Millimeter-wave observations appear to be a powerful tool for studying planetary atmospheres, from the point of view of thermal profile as well as chemical composition. Although some ambiguity in the interpretation remains, observations of CO on Mars allow one to derive information about the thermal profile at the time of dust storms, and to monitor possible short-term changes in CO abundance. However, millimeter-wave observations, even with large antennas, do not allow spatial resolution of the planets. Mapping of the thermal profile and of vertical distribution of the minor constituents, and monitoring them as a function of time, will be possible in the near future with millimeter interferometry. For the present, the infrared range has a great advantage in this respect, and infrared heterodyne spectroscopy, combined with simultaneous visible observations, could be the ideal tool for these purposes (Schrey *et al.* 1986).

ACKNOWLEDGMENTS

We are grateful to the technical staff of IRAM at Pico Veleta for their essential support during the observations, in particular to Haucke Hein and Santiago Navarro for the receiver tuning. We also thank R. Blundell for the October observations. We are indebted to Philipp James for providing information about the visual appearance of Mars at the time of our observations. E.L. thanks Daniel Gautier for his advice on the use of inversion methods. We thank Duane Muhleman and an anonymous referee for their comments which helped us to improve the paper considerably. S.A. acknowledges support received from NASA Grant NAGW-990.

REFERENCES

CHAHINE, M. T. 1968. Determination of the temperature profile in an atmosphere from its outgoing radiance. *J. Opt. Soc. Amer.* **58,** 1634–1637.

CLANCY, R. T., AND D. O. MUHLEMAN 1983. A measurement of the $^{12}CO/^{13}CO$ in the mesosphere of Venus. *Astrophys. J.* **273,** 829–836.

CLANCY, R. T., D. O. MUHLEMAN, AND B. M. JAKOSKY 1983. Variability of carbon monoxide in the Mars atmosphere. *Icarus* **55,** 282–301.

COMBES, F., E. FALGARONE, J. GUIBERT, AND NGUYEN-Q-RIEU 1980. CO observations of interstellar clouds: Isotopic ratios. *Astron. Astrophys.* **90,** 88–96.

GOOD, J. C., AND F. P. SCHLOERB 1981. Martian CO abundance from the $J = 0$–1 rotational transition: Evidence for temporal variations. *Icarus* **47,** 166–172.

GUELIN, M., J. CERNICHARO, C. KAHANE, AND J. GOMEZ-GONZALEZ 1986. A new free radical in IRC + 10216. *Astron. Astrophys.* **157,** L17–L20.

HESS, S. L., J. A. RYAN, J. E. TILLMAN, R. M. HENRY, AND C. B. LEOVY 1980. The annual cycle of pressure on Mars measured by Viking landers 1 and 2. *Geophys. Res. Lett.* **7,** 197–200.

HUNTEN, D. M. 1974. Aeronomy of the lower atmosphere of Mars. *Rev. Geophys. Space Phys.* **12,** 529–535.

KAKAR, R. K., J. W. WATERS, AND W. J. WILSON 1977. Mars: Microwave detection of carbon monoxide. *Science* **196,** 1090–1091.

KAPLAN, L. D., J. CONNES, AND P. CONNES 1969. Carbon monoxide in the Martian atmosphere. *Astrophys. J.* **157,** L187–L192.

KOLBE, W. F., H. BUSCHER, AND B. LESKOVAR 1977. Microwave absorption coefficients of atmospheric pollutants and constituents. *J. Quant. Spectrosc. Radiat. Transfer* **18,** 47–64.

KUTNER, M. L., AND B. L. ULICH 1981. Recommendations for calibration of millimeter-wavelength spectral line data. *Astrophys. J.* **250,** 341–348.

LELLOUCH, E., AND T. ENCRENAZ 1986. A study of planetary atmospheres in the submillimetric range. In *A Space-Borne Sub-Millimetre Astronomy Mission,* Segovia, Spain, 4–7 June 1986 (ESA SP260).

LIU, S. C., AND T. M. DONAHUE 1976. The regulation of hydrogen and oxygen escape from Mars. *Icarus* **28,** 231–246.

MARTIN, T. Z. 1974. The major Martian dust storms of 1971 and 1973. *Icarus* **23,** 108–115.

MARTIN, T. Z., AND P. B. JAMES 1987. The great dust storm of 1986(?). In *Mars: Evolution of Its Climate and Atmosphere,* LPI Technical Report 87-01.

MC ELROY, M. B., AND T. M. DONAHUE 1972. Stability of the Martian atmosphere. *Science* **177,** 986–988.

MC ELROY, M. B., T. Y. KONG, AND Y. L. YUNG 1977. Photochemistry and evolution of Mars atmo-

sphere: A Viking perspective. *J. Geophys. Res.* **82,** 4379.

MEERTS, W. L., F. H. DE LEEUW, AND A. DYNAMUS 1977. Electric and magnetic properties of carbon monoxide by molecular-beam electric resonance spectroscopy. *J. Chem. Phys.* **22,** 319–324.

POLLACK, J. B., D. S. COLBURN, F. M. FLASAR, R. M. KAHN, C. E. CARLSTON, AND D. PIDEK 1979. Properties and effects of dust particles suspended in the Martian atmosphere. *J. Geophys. Res.* **84,** 2729–2745.

SCHLOERB, F. P. 1985. Millimeter-wave spectroscopy of Solar System objects: Present and future. In *Proceedings of the ESO–IRAM–Onsala Workshop on (Sub)millimetre Astronomy*, Aspenas, Sweden, 17–20 June 1985.

SCHREY, U., H. ROTHERMEL, H. U. KAUFL, AND S. DRAPATZ 1986. Determination of the $^{12}C/^{13}C$ and $^{16}O/^{18}O$ ratio in the Martian atmosphere by 10 micron heterodyne spectroscopy. *Astron. Astrophys.* **155,** 200–204.

SEIFF, A. 1982. Post-Viking models for the structure of the summer atmosphere of Mars. *Adv. Space Res.* **2,** 3–17.

SEIFF, A., AND D. B. KIRK 1977. Structure of the atmosphere of Mars in summer at mid-latitudes. *J. Geophys. Res.* **82,** 4364–4378.

TRAUGER, J. T., AND J. I. LUNINE 1983. Spectroscopy of molecular oxygen in the atmospheres of Venus and Mars. *Icarus* **55,** 272–281.

VARANASI, P. 1975. Measurement of line widths of CO of planetary interest at low temperatures. *J. Quant. Spectrosc. Radiat. Transfer* **15,** 191–196.

WATSON, W. D., V. G. ANICICH, AND W. T. HUNTRESS, JR. 1976. Measurement and significance of the reaction $^{13}C^+ + {}^{12}CO \rightleftarrows {}^{12}C^+ + {}^{13}CO$ for alteration of the $^{12}C/^{13}C$ ratio in interstellar molecules. *Astrophys. J.* **205,** L165–L168.